SEISMIC ANALYSIS OF AN OFFSHORE WIND TURBINE ON THE MONOPOLE FOUNDATION USING THE TWO-STEP METHOD

Huynh Van Quan*, Le Huu Dat
Campus in Ho Chi Minh City, University of Transport and Communications

ARTICLE INFO

Received: 15/02/2024
Revised: 14/5/2024
Published: 14/5/2024

KEYWORDS

Offshore wind turbine
Monopile foundation
Seismic analysis
Two-step method
OpenSeesPL

ABSTRACT

This study employs a two-step method to examine the seismic response of offshore wind turbine (OWT) systems supported by monopile foundations. In the first step, the soil-monopile interaction (SMI) is simulated using the professional software program OpenSeesPL. In the second step, the OWT structure is simulated employing the lumped-parameter method (LMP). The response of the OWT structure is then analyzed using the results from the first step with a single degree of freedom (DOF). An OWT with a capacity of 5 MW is studied numerically. Three different soil profiles are analyzed, and the effects of ignoring soil-structure interaction (SSI) using fixed-base models are investigated. In comparison to the fixed-base model, the SMI increases the peak acceleration values of monopile tops: the ratios for dense sand, stiff clay, and multiple strata are 3.68, 2.62, and 2.58, respectively. Peak absolute displacements in the SSI model at the top of the tower are 10-20 times higher than those in a fixed-base model, and the SMI significantly contributes to absolute displacements.

PHÂN TÍCH TRỤ ĐIỆN GIÓ XA BỜ ĐẶT TRÊN MÓNG CỌC ĐƠN CHỊU ĐỘNG ĐẤT BẰNG PHƯƠNG PHÁP HAI BƯỚC

Huỳnh Văn Quân*, Lê Hữu Đạt
Phân hiệu tại Thành phố Hồ Chí Minh, Trường Đại học Giao thông vận tải

THÔNG TIN BÀI BÁO

Ngày nhận bài: 15/02/2024
Ngày hoàn thiện: 14/5/2024
Ngày đăng: 14/5/2024

TỪ KHÓA

Trụ điện gió xa bờ
Móng cọc đơn
Phân tích động đất
Phương pháp hai bước
OpenSeesPL

TÓM TẮT

Nghiên cứu này áp dụng phương pháp hai bước để khảo sát phản ứng của trụ điện gió ngoài khơi (OWT) đặt trên móng cọc đơn chịu tải trọng động đất. Trong bước một, tương tác giữa đất nền và móng được mô phỏng bằng phần mềm chuyên dụng OpenSeesPL. Bước thứ hai, hệ OWT được mô phỏng bằng phương pháp tham số tập trung. Trong phân tích, hệ OWT được mô hình thành một bậc tự do chịu kích thích nền là kết quả của bước một. Bài báo phân tích số đối với công trình OWT có công suất 5 MW. Ba môi trường đất đặt móng khác nhau được khảo sát và ảnh hưởng của việc bỏ qua tương tác kết cấu-đất nền đã được xem xét. So với mô hình cố định, tương tác giữa đất nền và móng (SFI) đã làm tăng giá trị gia tốc đỉnh móng. Tỷ lệ tăng tương ứng đối với cát chặt, sét cứng và đất nhiều lớp lần lượt là 3,68, 2,62 và 2,58. Việc xét đến SFI làm cho chuyển vị tuyệt đối của đỉnh tháp cao hơn 10-20 lần so với mô hình cố định. Trong đó, chuyển vị của hệ đất nền-móng đóng góp phần lớn vào giá trị chuyển vị tuyệt đối của đỉnh tháp.

DOI: https://doi.org/10.34238/tnu-jst.9704

* Corresponding author. *Email: quanhv_ph@utc.edu.vn*

1. Introduction

Wind energy sources are becoming more and more widespread worldwide. In Vietnam, onshore wind farms like those in Quang Tri, Dak Nong, and Ninh Thuan provinces are highly popular. Offshore wind farms like Ben Tre, Bac Lieu, Ca Mau, and other provinces have grown over time [1], [2]. Onshore wind turbine foundations are relatively easy to design and build because they are standardized and well-known to civil engineers. On the other hand, because they have to match the seabed's soil and the sea level's depth, the foundations of OWTs have special characteristics and are extremely complex. Sea reclamation projects to construct OWTs have become very important due to future demands [3].

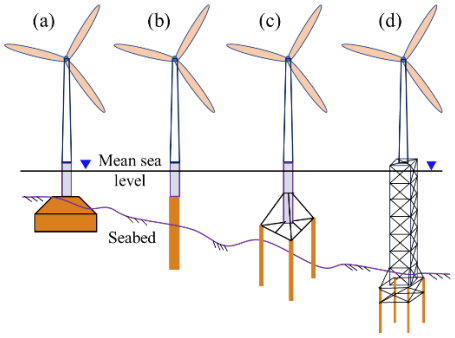

Figure 1. *Options for OWT's foundation, (a): gravity, (b): monopile, (c): tripod, (d): jacket*

According to Gasch [4], foundation work accounts for 20 to 30 percent of a wind power project's overall cost. Due to the high cost, it is important to select a foundation that suits the actual conditions. For OWTs, a variety of foundation types have been employed, such as gravity, monopile, tripod, and jacket foundations (see Figure 1) [5]. The most common foundation type, monopile foundations, not only offer cost efficiencies but also guarantee operational safety. According to Oh [6], a significant 91% of projects implemented in 2014 employed monopile foundations. Forecasts indicate that between 50 and 60 percent of OWTs will be built with monopile foundations by 2020 [7]. For example, a 5 MW OWT installed in the North Sea was reported by [8] to have a tower height of 95 m above mean sea level and a rotor diameter of 125 m. The corresponding static forces of wave and wind in an OWT at the seabed were 4 MNm for torsional moments, 35 MNm for axial loads, and 16 MN for horizontal loads. These numbers demonstrate that in order for the monopile to respond to an external force, it must produce an extremely high resistance. For this reason, researching OWTs with monopile foundations is highly helpful.

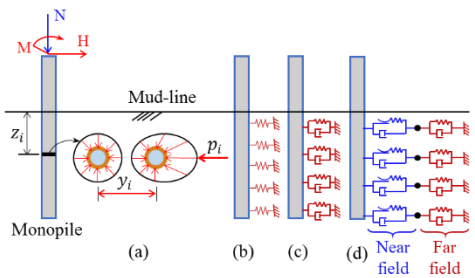

Figure 2. *P-y curve models* [9], [10]

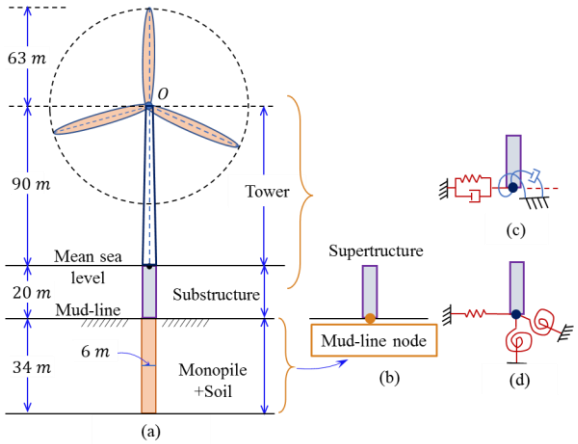

Figure 3. *Sway-rocking models* [11], [12]

A brief summary of two popular LMP for monopile foundations can be found in Figures 2 and 3. P-y curve method (refer to Figure 2(a)) divides the soil-monopile system into smaller elements. All elements of the monopile are connected to the ground along its length by either a soil spring (refer to Figure 2(b)); a couple of springs and dampers (refer to Figure 2(c)); or, in a more complex connection, a division of the surrounding soil into near and far fields (refer to Figure 2(d)) [9], [10]. The monopile and soil systems' responses are replaced in sway-rocking methods by a mud-line node at the seabed (see Figure 3(a)). The mud-line node, as seen in Figure 3(b,c), has six DOFs in the spartial model but only basic DOFs in the plane model [11], [12]. The difficulty in simulating the nonlinearities of SMI is the LMP's limitation.

In the finite-element method (FEM), the authors used ABAQUS [13] or FAST software [11] to model and calculate the OWT responses. In these models, a significant amount of simulation and computation will be needed to model the entire OWT system (soil, foundation, substructure, tower, hub, rotor, nacelle,...).

In seismic analysis of an OWT, the SMI is complicated, while we aim to obtain the specific responses of the OWT superstructure. Consequently, it will be very helpful to reduce computations if SMI and tower structure can be modeled separately. The suggestion is then that the tower structure should be simulated by the LMP and the SMI by the FEM. This analysis process is consistent with the suggestion that SSI problems be solved using Kausel's superposition method (two-step method) [14] - [16].

This paper employs the two-step method for seismic analysis of the soil, monopile foundation, and OWT systems. By including the SMI, the analysis results are more in line with the real behavior. The first step of this method is to analyze the SMI using OpenSeesPL. In the second step, the tower structure at its base is excited using the accelerations from the first step. In order to simulate the tower, the system of hub, nacelle, and blades are combined into a single lump at hub height. Meanwhile, the tower, which is a massless structure, is modeled using an Euler-Bernoulli beam model. In the numerical calculation, the SMI examines homogeneous soil of dense sand and stiff clay, multiple strata; the monopile length is 34 m, and the OWT has a capacity of 5 MW. The analytical results are compared to the fixed-base model.

2. The two-step method to OWT seismic analysis

The paper proposes solving the SSI problem of an entire OWT system in two steps using Kausel's method [14] - [16] (see Figure 4). The SMI under seismic load (Figure 4(a)) is analyzed by matrix equation (2) in the first step, which ignores the mass of the structure (Figure 4(b)). The acceleration at the top of the monopile foundation is obtained in this step, which causes the structure to vibrate in the second step. In order to obtain the responses from the OWT system (Figure 4(c)), the analysis process in the second step is performed using matrix equation (2). In seismic analysis, the first and second steps are referred to as kinematic and inertial interactions, respectively. Matrix equation (3), which is the product of matrix equations (1) and (2), serves as the general equation of motion for the analysis of the entire OWT system.

$$\boldsymbol{M_1\ddot{u}_1 + C\dot{y}_1 + Ky_1 = 0} \quad (1)$$

$$\boldsymbol{M\ddot{y}_2 + C\dot{y}_2 + Ky_2 = -M_2\ddot{u}_1} \quad (2)$$

$$\boldsymbol{M\ddot{u} + C\dot{y} + Ky = 0} \quad (3)$$

where the relative and absolute displacement vectors of the foundation are denoted by $(\boldsymbol{y_1}, \boldsymbol{u_1})$; the relative displacement vector of the structure is denoted by $\boldsymbol{y_2}$; the ground motion vector is denoted by $\boldsymbol{u_g}$; the mass of the soil matrice is omitted by $\boldsymbol{M_2}$, while the mass matrice of the structure is omitted by $\boldsymbol{M_1}$; $\boldsymbol{u_1 = y_1 + u_g}$, $\boldsymbol{u = u_1 + y_2}$, $\boldsymbol{y = y_1 + y_2}$, and $\boldsymbol{M = M_1 + M_2}$; the absolute and relative displacement vectors are represented by $\boldsymbol{u}$ and $\boldsymbol{y}$, respectively; and the mass, damping, and stiffness matrices of the entire system are denoted by $\boldsymbol{M}$, $\boldsymbol{C}$ and $\boldsymbol{K}$. The equations (1)-(3) have displacement vectors $(\boldsymbol{u, y, u_g, u_1, y_1, y_2})$ with size $1 \times n$; and matrices of

mass ($\boldsymbol{M}, \boldsymbol{M_1}, \boldsymbol{M_2}$), stiffness ($\boldsymbol{K}$), and damping ($\boldsymbol{C}$) with size $n \times n$; where n is the DOF number of the entire OWT system. It should be noted that corresponding elements in vectors ($\boldsymbol{u_1}, \boldsymbol{y_1}, \boldsymbol{y_2}$) and matrices ($\boldsymbol{M_1}, \boldsymbol{M_2}$) will have zero values if any mass of DOF is ignored.

Using a finite element tool is recommended for the first step, as per [14] – [16]. At the present time, a number of commercial programs, including ABAQUS, ANSYS, PLAXIS, and others, can perform SFI due to advances in computer software. A free finite-element software called OpenSeesPL was created by the Pacific Earthquake Engineering Research Center (University of California) to analyze the lateral 3D ground-pile interaction [17]. It is an effective technique to analyze nolinear SMI under earthquake loads. OpenSeesPL supplies pushover, mode shape, and base input acceleration analysis as available analysis options. More information about the program can be found in the OpenSeesPL user manual. In this paper, a SMI is simulated with OpenSeesPL; the OWT tower system is modeled by either a single DOF system (if tower mass is ignored) or a multi-DOF system [18].

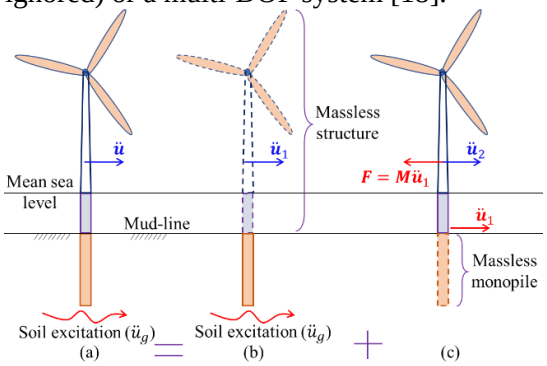

Figure 4. *(a): the complete solution, (b): the first step, and (c): the second step*

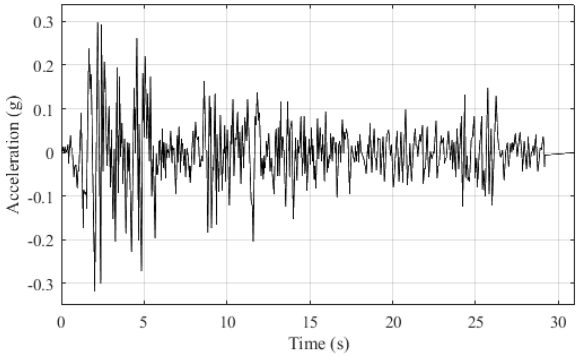

Figure 5. *Acceleration of the El Centro (1940) earthquake* [21]

3. Numerical studies and discussion

3.1. Description

This study examines a 5-MW OWT using the model shown in Figure 3(a). The hub diameter is 3 m, the hub height is 90 m, and the rotor diameter with three blades measures 126 m. The mass of the tower is 347 tons, the nacelle is 24 tons, and the rotor is 110 tons. It is assumed that the tower and substructure were modeled with constant dimensions of 6 m in diameter and 0.019 m in thickness. The monopile has a diameter of 6.0 meters, a wall thickness of 0.09 meters, and an embedment depth of 34 meters into the soil strata [19], [20]. The tower and substructure were defined by linear elastic material properties and elastic Euler-Bernoulli beam elements. The monopile foundation is placed on three different soil types (Cases 1-3) with a 66-meter soil depth. The soils in Cases 1 and 2 are homogeneous, composed of stiff clay and dense sand. Case 3 has multiple strata arranged as follows: 6 m-dense sand, 10 m-medium clay, and 50 m-stiff clay. Table 1 lists the predefined parameters for different soils. The longitudinal El Centro (1940) [21] with $0.319g$ in PGA and $g = 9.81$ m/s^2 is the input motion ($\ddot{\boldsymbol{u}}_{\boldsymbol{g}}$); see Figure 5.

Table 1. *Parameter values of soils* [17]

Soil type	Shear wave velocity (m/s)	Friction angle/ Undrained shear strength (kPa)	Possion's ratio	Mass density (kg/m^3)
Dense sand	255	40.0^o	0.4	2.1×10^3
Medium clay	200	37.0	0.4	1.5×10^3
Stiff clay	300	75.0	0.4	1.8×10^3

3.2. Analysis technique

As previously indicated, the OpenSeesPL program is employed for performing the seismic analysis of SMI in the first step. The seismic analysis of the SMI involves three steps. The model parameters, material properties, and mesh parameters of the soil and pile strata are defined in the step 1. There is a menu with 18 predefined cohesionless and cohesive soil materials that users can choose from. In addition, OpenseesPL allows users to define the properties of sand and clay. In this study, the default properties of the predefined soils from OpenSeesPL were applied, see Table 1. Rayleigh damping, plastic material, and an 8-node brick element were employed to simulate the soils. For boundary conditions, rigid bedrock and rigid box types were selected. In step 2, the paper chose the option for a single motion analysis. El Centro (1940) in Figure 5, which has a longitudinal direction and a scale factor of 1.0, is the time-history acceleration of the input motion. Step 3 performs finite element analysis to get the acceleration of the structure base (the top of the monopile, $\ddot{u}_1$); these results are presented in Section 3.3.

The OWT model used in this study has a single DOF, and the mass of the blades and rotor-nacelle is combined to equal 350 tons at the top of the tower model. The substructure and tower mass are neglected, and the blades are not modeled [20]. Elastic Euler-Bernoulli beam elements with linear elastic material properties and a structural Rayleigh damping assumption of ξ=1.0% were applied to model the tower and substructure [22]. The vector form of equation (2) in the second step, which matches to the single DOF of an OWT system, is as follows:

$$m_2\ddot{y}_2 + c\dot{y}_2 + ky_2 = m_2\ddot{u}_1 \quad (4)$$

where the mass of the rotor-nacelle and blades $m_2 = 240 \times 10^3 + 110 \times 10^3 = 350 \times 10^3$ kg, flexural stiffness of $EI = 1.04 \times 10^{12}$ Nm^2 [23], hub height $H_{hub} = 90$ m, substructure height $h = 20$ m, monopile tower total length $H = H_{hub} + h = 110$ m, $k = \frac{EI\pi^4}{32H^3} = 2.53 \times 10^9$ N/m, $c = 2\xi\sqrt{k.m} = 2 \times 0.01\sqrt{(2.53 \times 10^9)(350 \times 10^3)} = 0.6 \times 10^6$ Ns/m.

3.3. The first step results: responses of soil-monopile system

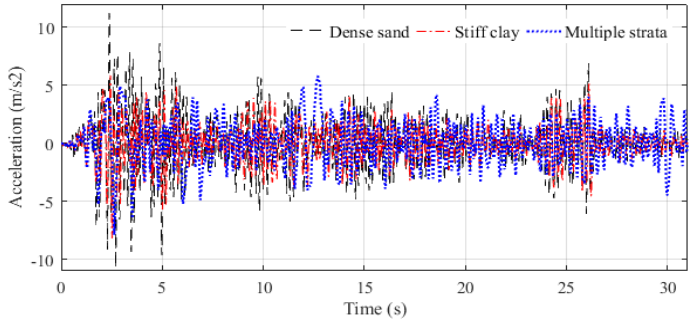

Figure 6. *The accelerations ($\ddot{u}_1$) of the monopile top with different soil profile*

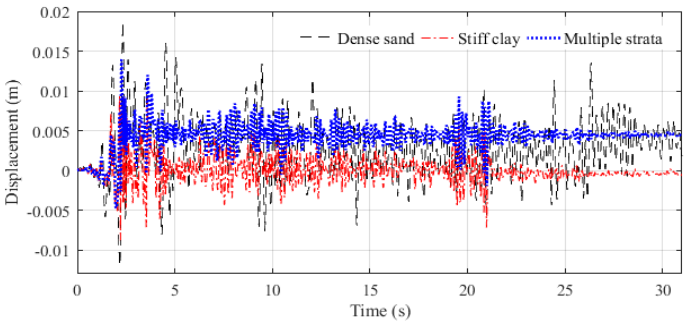

Figure 7. *The displacements (u_1) of the monopile top with different soil profile*

The responses of the monopile top, acceleration $\ddot{u}_1$ and displacement u_1, from the OpenSeesPL seismic analysis of the SMI are shown in Figure 6 and 7. The monopile's responses are influenced by soil profiles; these responses are displayed on a graph to facilitate observation.

Figure 6 shows that the acceleration history of Case 3 (multiple strata) is reducing more slowly than that of Cases 1-2. Case 2 (stiff clay) had the least displacement from the zero axis of displacement because of its high elasticity; this was due to the monopile top's permanent deformation under seismic loads; see Figure 7. Table 2 tabulates the peak values of these responses.

Table 2. *Peak responses for the monopile tops*

Case	Acceleration (m/s^2)			Displacement
	Present, (1)	***Fixed base, (2)***	***Ratio,*** $(1)/(2)$	**(m), (3)**
1	11.52	$0.319g$	3.68	18.72×10^{-3}
2	8.21		2.62	9.41×10^{-3}
3	8.09		2.58	13.88×10^{-3}

As compared to the fixed model (El Centro), the results in Table 2's column (1) demonstrate that the SMI significantly increases peak acceleration values. The ratios for Cases 1-3 are 3.68, 2.62, and 2.58, respectively; Case 1 (dense sand) has the highest ratio. The ratios of Case 1 to Cases 2–3 were $11.52/8.21 = 1.40$ and $11.52/8.09 = 1.42$ times, in that order. If we assume that the tower and substructure are made of rigid bars, then the values in column (3) represent their peak displacements.

3.4. The second step results: responses of wind turbine tower

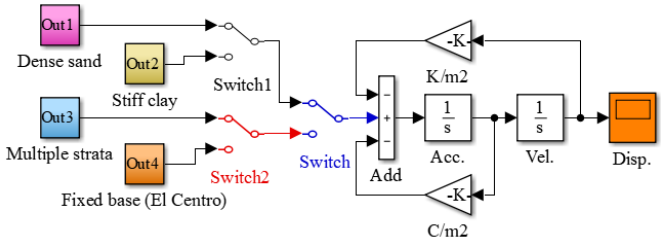

Figure 8. *Matlab-Simulink diagram for analyzing the second step*

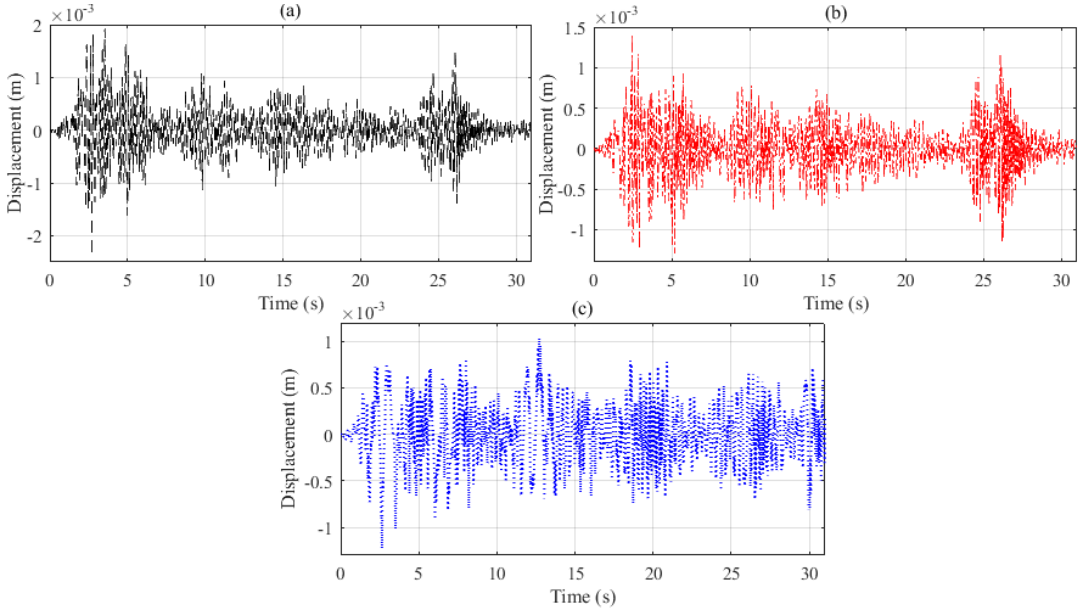

Figure 9. *The relative displacement of the tower top (a): dense sand, (b): stiff clay, (c): multiple strata*

Using the Runge-Kutta method of the Matlab-Simulink diagram in Figure 8, where $\ddot{u}_1$ has been identified in Figure 6, is the second step in integrating equation (4). The relative tower top displacements from the second-step analysis are shown in Figure 9. By adding the relative displacements in Figure 9 to the foundation displacements in Figure 7, one gets the absolute displacements of the tower tops as in Figure 10.

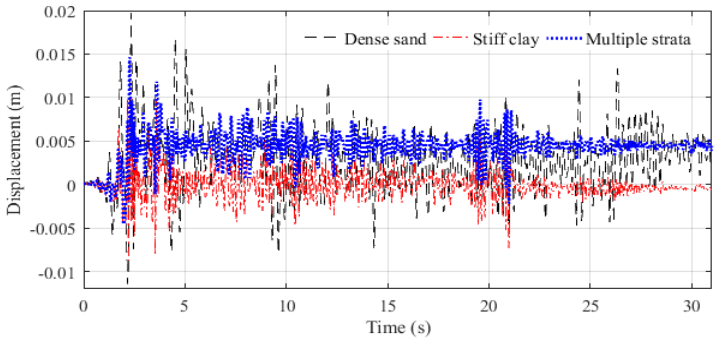

Figure 10. *The absolute displacement of the tower top in the present*

In the case of fixed-base models, ignoring the effects of SMI, the ground acceleration of El Centro (1940) occurs directly at the structure's base. After that, equation (4) is examined using the acceleration formula, $\ddot{u}_1 = \ddot{u}_g$, yielding the tower top displacement shown in Figure 11. The peak values of the second-step displacements are tabulated in Table 3.

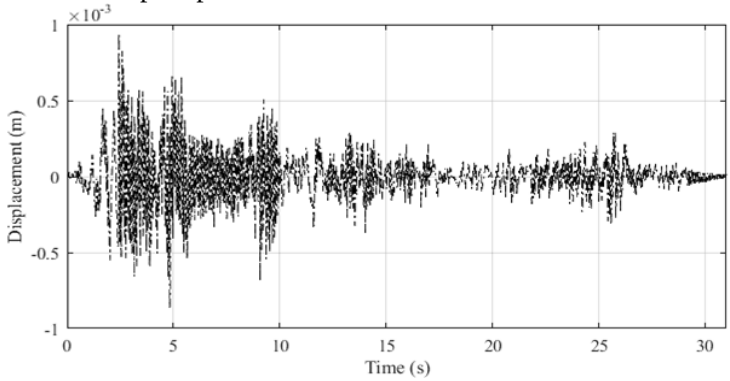

Figure 11. *The displacement of the tower top in the fixed-base model*

Table 3. *The peak displacements of tower tops*

Case	Relative disp. (m), (1)	Absolute disp. (m), (2)	Fixed base (m), (3)	Ratio, $(4) = (1)/(3)$	Ratio, $(5) = (2)/(3)$
1	2.39×10^{-3}	19.64×10^{-3}		2.54	20.89
2	1.41×10^{-3}	9.84×10^{-3}	0.94×10^{-3}	1.50	10.47
3	1.23×10^{-3}	14.63×10^{-3}		1.31	15.56

The results in Table 2 and 3 show that, due to the high stiffness of the tower and substructure, the relative displacement of the tower top is minimal (1.3-2.5 times larger than a fixed-base model). The SMI is a major contributor to absolute displacements. Since the displacements are 10–20 times larger than those of a fixed-base model, Column (5) of Table 3 shows that SSI cannot be ignored in the seismic analysis of an OWT system.

4. Conclusions

The study employed a two-step method to investigate the response of OWT systems situated on monopile foundations under seismic loading. At the first step, the authors employed OpenSeesPL, a professional software program, to simulate SMI. The results of the first step were

utilized as the input for tower analysis in the second step. The numerical investigation examined three different soil profiles: dense sand, stiff clay, and multiple strata. The SMI increases the peak acceleration values of the tops of monopiles in dense sand, stiff clay, and multiple strata by factors of 3.68, 2.62, and 2.58, respectively. Peak absolute displacements in the SSI model were 10–20 times higher at the top of the tower than in the fixed-base model. One of the paper's limitations is the absence of a comparison between the FEM methods and the present analysis. It is recommended that SSI be taken into account when analyzing OWTs; more investigation is needed with different soils and foundations; and to find the correlation coefficient of responses between the SSI model and the fixed-base model to minimize computation costs.

Acknowledgment

This research is funded by University of Transport and Communications (UTC) under grant number T2024-PHII_CT-006.

REFERENCES

[1] 4coffshore Company, "Offshore Wind farms in Vietnam," 2024. [Online]. Available: https://www.4coffshore.com/ windfarms/vietnam/. [Accessed Feb. 14, 2024].

[2] V. Q. Huynh and H. T. Tran, "Analytical solution of monopile-based offshore wind turbines under dynamic loads," *TNU Journal of Science and Technology*, vol. 227, no. 11: Natural Sciences - Engineering - Technology, pp. 222-229, 2022.

[3] T. Dung, "Viet Nam offshore wind power sparks influx of foreign investment: Nikkei Asia," Vietnam Government News, 2023. [Online]. Available: https://en.baochinhphu.vn/viet-nam-offshore-wind-power-sparks-influx-of-foreign-investment-nikkei-asia-111230116145508058.htm. [Accessed Feb. 14, 2024].

[4] R. Gasch and J. Twele, *Wind power plants: fundamentals, design, construction and operation,* Springer Science & Business Media, 2011.

[5] F. Miceli, "Offshore wind turbines foundation types," 2012. [Online]. Available: http://www.windfarmbop.com/ tag/monopile/. [Accessed Feb. 14, 2024].

[6] K. Y. Oh, W. Nam, M. S. Ryu, *et al.,* "A review of foundations of offshore wind energy convertors: Current status and future perspectives," *Renewable and Sustainable Energy Reviews*, vol. 88, pp. 16-36, 2018.

[7] B. C. O'Kelly and M. Arshad, "Offshore wind turbine foundations–analysis and design," in *Offshore Wind Farms*, Woodhead Publishing, 2016, pp. 589-610.

[8] K. Lesny and J. Wiemann, "Design aspects of monopiles in German offshore wind farms," in *Proc. of the Inter. Symp. on Frontiers in Offshore Geotechnics*, AA Balkema Publishing, 2005, pp. 383-389.

[9] M. H. E. Naggar and K. J. Bentley, "Dynamic analysis for laterally loaded piles and dynamic p-y curves," *Canadian Geotechnical Journal*, vol. 37, no. 6, pp. 1166-1183, 2000.

[10] E. V. Buren and M. Muskulus, "Improving pile foundation models for use in bottom-fixed offshore wind turbine applications," *Energy Procedia*, vol. 24, pp. 363-370, 2012.

[11] S. Jung, S. R. Kim, and A. Patil, "Effect of monopile foundation modeling on the structural response of a 5-MW offshore wind turbine tower," *Ocean Engineering*, vol. 109, pp. 479-488, 2015.

[12] C. Sun and V. J. M. S. Jahangiri, "Bi-directional vibration control of offshore wind turbines using a 3D pendulum tuned mass damper," *Mechanical Systems and Signal Processing*, vol. 105, pp. 338-360, 2018.

[13] M. Wang, Y. Zhao, W. Du, *et al.,* "Derivation and validation of soil-pile-interaction models for offshore wind turbines," in *ISOPE Inter. Ocean and Polar Eng. Conf.*, 2013, pp. ISOPE-I-13-091.

[14] E. Kausel, R. V. Whitman, J. P. Morray, *et al.,* "The spring method for embedded foundations," *Nuclear Engineering and Design*, vol. 48, pp. 377-392, 1978.

[15] V. Q. Huynh and X. H. Nguyen, *Seismic soil-structure interaction: Theory and Experiment,* Hanoi: Transport Publishing House, (in Vietnamese), 2023.

[16] V. Q. Huynh, "Seismic analysis of a soil-liquid tank system using the two-step method," *Transport and Communications Science Journal,* vol. 75, no. 4, pp. 1-14, 2024.

[17] SoilQuake.net website, "Geotechnical/SSI simulation tools," 2022. [Online]. Available: http://www.soilquake.net/. [Accessed Feb. 14, 2024].
[18] W. C. Ray and P. Joseph, *Dynamics of Structures*, 3th ed. Berkeley: Com. & Stru., Inc., 1995.
[19] J. Jonkman, S. Butterfield, W. Musial, *et al.,* "Definition of a 5-MW reference wind turbine for offshore system development," *Technical Report,* no. NREL/TP-500-38060, 2009.
[20] W. Carswell, J. Johansson, F. Løvholt, *et al.,* "Foundation damping and the dynamics of offshore wind turbine monopiles," *Renewable Energy*, vol. 80, pp. 724-736, 2015.
[21] Vibrationdata.com website, "El Centro earthquake page," 2000. [Online]. Available: http://www.vibration data.com/elcentro.htm. [Accessed Feb. 14, 2024].
[22] A. Malekjafarian, S. Jalilvand, P. Doherty, *et al.,* "Foundation damping for monopile supported offshore wind turbines: A review," *Marine Structures*, vol. 77, 2021, Art. no. 102937.
[23] G. B. Colherinhas, F. Petrini, M. V. G. Morais*, et al.,* "Optimal design of passive-adaptive pendulum tuned mass damper for the global vibration control of offshore wind turbines," *Wind Energy*, vol. 24, no. 6, pp. 573-595, 2021.